Journal of Alloys and Compounds, 195 (1993) 535–542
JALCOM 7522

Surface stability of superconducting oxides

W R Flavell[a], D R C Hoad[a], A J Roberts[a], R G Egdell[b], I W Fletcher[c] and G Beamson[c]

[a]Department of Chemistry, UMIST, PO Box 88, Manchester M60 1QD, UK

[b]Inorganic Chemistry Laboratory, University of Oxford, South Parks Road, Oxford, OX1 3QR, UK

[c]ICI Wilton Research Centre, PO Box 90, Wilton, Middlesbrough, Cleveland, TS6 8JE, UK

Abstract

One factor which may limit the scale of application of oxide superconductors is their intrinsic instability when in contact with air containing water vapour. All families of these materials are to some extent subject to surface degradation reactions to form insulating products. These reactions may be monitored conveniently by surface sensitive techniques such as photoemission. Here we show examples of the application of this technique to degradation reactions occurring in ceramic and single crystal material, and initial results from superconducting tapes. Systems studied include $YBa_2Cu_3O_{7-x}$, $Bi_2Sr_2CaCu_2O_{8+x}$ and $BaPb_{1-x}Bi_xO_3$. For the latter, we show that the extent of degradation is sensitively dependent on the chemical composition, with metallic compositions being dramatically more unstable than non-metallic compositions.

Amongst the degradation products formed from materials containing Ba, Sr or Ca is the alkaline earth carbonate. This is formed by reaction with CO_2 in a reaction catalysed by water vapour. The carbonate is particularly stable in the case of Ba, and this may go some way towards explaining the rapid rates of degradation of $YBa_2Cu_3O_{7-x}$ and $BaPb_{1-x}Bi_xO_3$, when compared with $Bi_2Sr_2CaCu_2O_{8+x}$.

1. Introduction

In the years following the discovery of high temperature superconducting oxides, it has become clear that these complex oxide materials tend to undergo "degradation" when in contact with air containing water vapour, which in the worst cases may destroy the superconducting properties of the oxide.

Although these reactions threaten to limit the scale of application of these materials, they remain rather poorly understood. Degradation occurs at the surfaces of the material exposed to the atmosphere. The process occurs much faster for poor quality ceramics than for dense ceramics or well-oriented thin films, and this may be associated with faster grain boundary diffusion in the former case. Because of its surface nature, the process may be studied conveniently by surface-sensitive techniques, such as photoemission. Here we describe some of our work using XPS and valence level photoemission, supplemented by FTIR spectroscopy, aimed at studying degradation processes as a function both of environment, and of chemical composition of the oxide. We show that in some cases, the behaviour towards degradation may be linked to the electronic structure of the material.

2. Degradation of $YBa_2Cu_3O_{7-x}$

Like many other oxides, high-temperature superconductors are susceptible to reaction with atmospheric CO_2 and H_2O to give insulating products, including surface carbonate and hydroxide species [1-6]. The degradation reaction of $YBa_2Cu_3O_7$ is perhaps the best studied [1,3], with the dominant reaction now established as

$$2YBa_2Cu_3O_7 + 3CO_2 \longrightarrow Y_2BaCuO_5 + 3BaCO_3 + 5CuO + 0.5O_2$$

at the synthesis temperature of 950°C [3], possibly changing to

$$2YBa_2Cu_3O_7 + 4CO_2 \longrightarrow 4BaCO_3 + Y_2Cu_2O_5 + 4CuO + 0.5O_2$$

at lower temperatures [3]. These reactions are strongly catalysed by the presence of water vapour [7].

The presence of degradation products at the surface of the material has a very strong effect on both core-level and

0925-8388/93/$06.00

valence-level photoemission spectra. In the case of core-level spectra, the effect is probably most dramatic on the shape of the O 1s core level peak; this initially contributed considerably to controversy in the literature concerning the detailed interpretation of this peak shape [1].

The strong surface sensitivity of photoemission (where the electron mean free pathlength may only be of the order of 15Å [8]) means that techniques such as XPS may be used to monitor sensitively the appearance of degradation products. The technique shows that the build-up of contaminant phases may be rapid on the photoemission depth scale under ambient conditions; an example is shown in figure 1, where the O 1s peak shapes from XPS are shown for $YBa_2Cu_3O_{7-x}$ ceramics stored under different conditions. The shape of the O 1s peak measured from a variety of superconducting oxides has been a subject of intense controversy. We have reviewed the literature on this topic on a number of occasions [1,9], and a detailed discussion is beyond the scope of this paper. However, it is widely accepted that the structure at around 528-529 eV is intrinsic to the superconductor, whereas much of the intensity at around 531 eV can be attributed to an extrinsic surface component [1], whose size is enhanced in grazing emission [1]. In "as-presented" samples, the size of this feature increases with time following synthesis, and corresponding changes are seen in the Ba 3d and C 1s (CO_3^{2-}) parts of the spectrum [7], leading us to suppose that much of this intensity is due to build up of products of the degradation reaction, including $BaCO_3$. Annealing inside the XPS spectrometer in 1 bar pure oxygen at high temperature leads to the almost complete removal of this high binding energy feature [7]. As this treatment mimics the initial synthesis conditions, this leads us to the conclusion that the quite strong contamination shown in figure 1(a) is likely to have been produced during the short exposure of the ceramic to the atmosphere between removal from the synthetic furnace and insertion into the XPS spectrometer. If we assume that the contaminant overlayer is laterally homogeneous, integration of the XPS flux attenuation expression allows us to make an

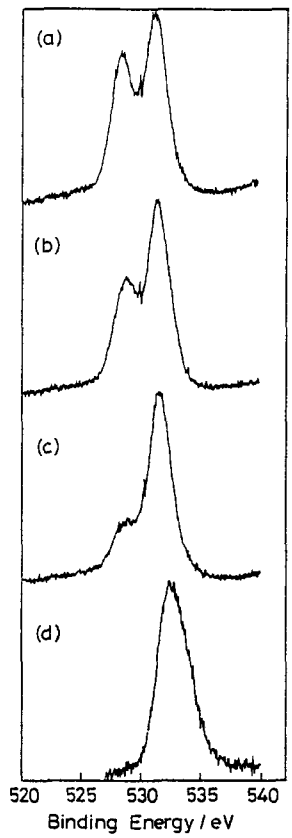

Figure 1. O 1s XPS of $YBa_2Cu_3O_{7-x}$ as a function of storage conditions (a) after around ten minutes' exposure to atmosphere following synthesis, (b) after 51 days' storage in a stoppered glass tube, (c) after 126 days as (b), (d) after 100 days' exposure to atmosphere.

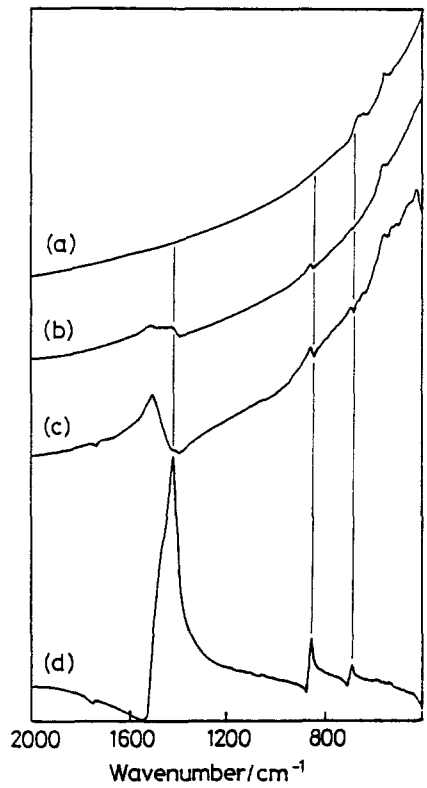

Figure 2. IR reflectance spectra for polycrystalline $YBa_2Cu_3O_{7-x}$ (a) as prepared, (b) after exposure to water vapour saturated air at 21°C for 21 hr, (c) as (b) but after 92 hr, (d) IR reflectance of $BaCO_3$. Note the gradual appearance of bands due to $BaCO_3$ in the superconductor spectra.

estimate of the depth of this overlayer of around 12Å, rising to around 60Å for the sample shown in figure 1(d) [7].

Further support for the presence of $BaCO_3$ comes from FTIR specular reflectance spectroscopy, where the strong Reststrahlen bands due to the internal modes of the carbonate anion (at 693 cm^{-1}, 855 cm^{-1} and 1445 cm^{-1}) are seen to appear in the spectra as a function of time when $YBa_2Cu_3O_{7-x}$ ceramics are exposed to saturated water vapour (figure 2). It is noticeable that the new features introduced by carbonate build-up correspond to dips in reflectivity at positions corresponding to the band maxima of the internal CO_3^{2-} anion modes. This is as expected, as the effect of a dielectric layer (the contaminants) on a metallic substrate (the superconductor) is to produce dips in the IR reflectivity at the LO phonon frequencies of the overlayer [7,10]. The assignment to $BaCO_3$ has been further confirmed by Raman spectroscopy, where bands due to $BaCO_3$ (and Y_2BaCuO_5) are clearly observed [7].

Experiments of this type carried out on reduced, non-superconducting material ($x \approx 1$) appear to indicate that the rates of degradation are not appreciably different for the superconducting (metallic) and non-superconducting (semiconducting) materials [7]. (This is, however, somewhat difficult to quantify, as the rising background of high metallic reflectance in the superconductor spectrum (figure 2 (a)) is absent for the semiconductor).

3. Degradation of $BaPb_{1-x}Bi_xO_3$

Less well-studied superconducting oxides, such as those which contain no copper also appear to show some surface instability. Indeed, one reason for the paucity of photoemission data from the $BaPb_{1-x}Bi_xO_3$ system is the marked instability of freshly prepared surfaces of this material to degradation in UHV [11,12]. The difficulties associated with producing clean, stable and representative surfaces of this material and associated materials such as $Ba_{1-x}K_xBiO_3$ [13] and $Ba_{1-x}Rb_xBiO_3$ [14,15] have been noted in the literature.

Our own work in this area stems from the observation that the rate of appearance of features associated with surface degradation in valence band photoemission seems to be very sensitively dependent on the Bi:Pb ratio in the $BaPb_{1-x}Bi_xO_3$ system [11]. The material is superconducting only in the composition range $0.05 \leq x \leq 0.3$, with a maximum T_c of around 13K at $x=0.25$ [16]. The system undergoes a charge density wave- (CDW-) driven transition to a semiconducting state at $x \approx 0.4$ [17]. The rate of degradation of freshly prepared surfaces in UHV appears to be very closely linked to the metal-to-semiconductor transition, with the surfaces of semiconducting compositions appearing relatively stable, whilst those of metallic compositions undergo a very rapid degradation at room temperature, possibly by reaction with components of the residual vacuum, such as H_2O [11].

In order to investigate this further, we have performed an XPS investigation of ceramics in the $BaPb_{1-x}Bi_xO_3$ system which have undergone an accelerated degradation process, involving exposure to air saturated with water vapour for extended periods. Figures 3 and 4 show XPS in the Ba 3d region for degraded x=0.5 (semiconducting) and x=0.3 (metallic) compositions. These compositions are chosen to lie close to, but on either side of the metal-to-non-metal transition. In both cases, the samples were exposed to air saturated with water vapour for a period of 35 days.

In figure 3, which shows the spectra for the semiconducting composition, it can be seen that the Ba 3d feature is split into the expected spin-orbit-split multiplet, corresponding to Ba $3d_{5/2}$ and Ba $3d_{3/2}$ peaks. However, a small asymmetry is seen on the high binding energy side of each of the main features, and this appears to show a slight increase in relative intensity on moving from normal to 20° emission angle (relative to the surface), suggesting that the feature is due to some form of contaminant overlayer. A very different spectral profile is seen in the case of the degraded x=0.3 sample (figure 4), where very strong high binding energy features are observed, in addition to the Ba signal from $BaPb_{1-x}Bi_xO_3$ itself. The intensity of the high binding energy features are strongly increased in grazing (20°) emission, becoming the dominant peaks. This suggests that the surface is strongly contaminated with a new, Ba-containing phase. One obvious contender is again $BaCO_3$. Support for this idea comes from corresponding changes in the O 1s region of the spectrum and the observation in the C 1s region of the spectrum of a well-defined CO_3^{2-} C 1s line [11,18], and in addition from the IR reflectance spectra which reveal the presence of strong Reststrahlen bands associated with the internal vibrations of the CO_3^{2-} anion in the spectra of degraded pellets [11,19]. We conclude, therefore, that one of the degradation products of $BaPb_{1-x}Bi_xO_3$ is $BaCO_3$, as for $YBa_2Cu_3O_{7-x}$.

It is tempting to associate the rather facile decomposition of both these materials with the very high thermodynamic stability of $BaCO_3$. One important difference between the two systems, however, is that in the case of $YBa_2Cu_3O_{7-x}$, the rate of degradation does not appear to be very dependent on whether the sample is

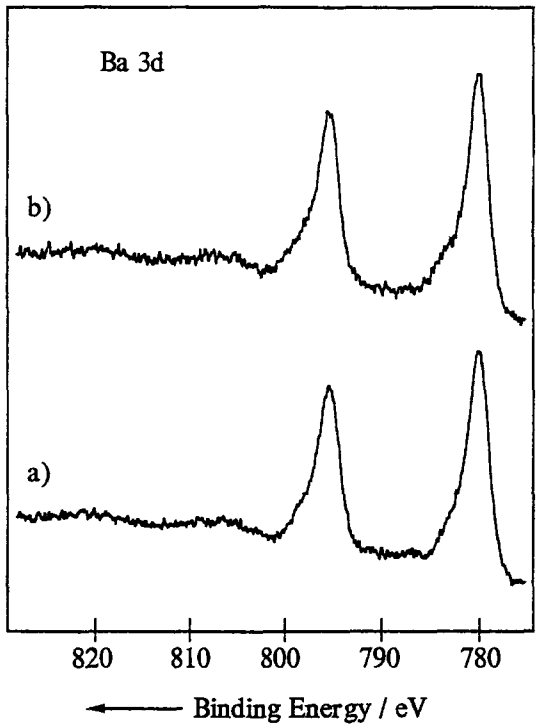

Figure 3. Ba 3d region XPS for $BaPb_{0.5}Bi_{0.5}O_3$ (semiconducting), following accelerated degradation, a) normal emission, b) grazing emission (angle of emission ≈ 20° to surface, enhanced surface sensitivity). Note the small high binding energy shoulders to the main peaks.

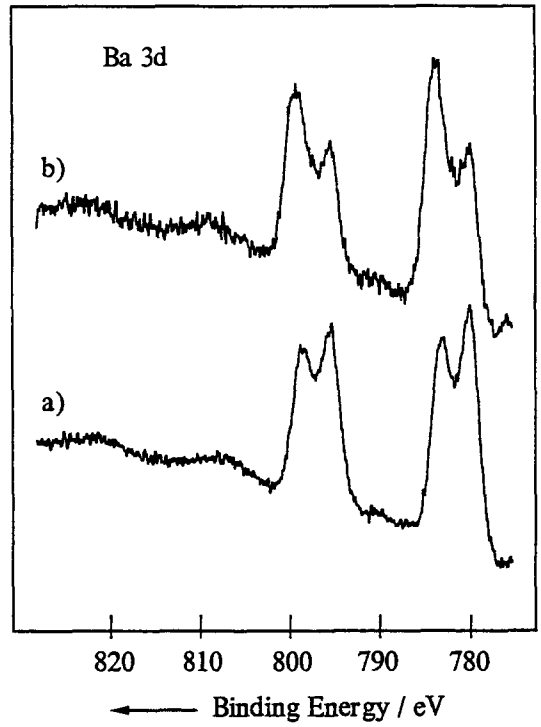

Figure 4. Ba 3d region XPS for $BaPb_{0.7}Bi_{0.3}O_3$ (metallic) following accelerated degradation, a) normal emission, b) grazing emission (angle of incidence ≈20° to surface, enhanced surface sensitivity). Note the intense high binding energy features, which are strongly enhanced in grazing emission.

semiconducting or superconducting, whilst for $BaPb_{1-x}Bi_xO_3$ metallic (and superconducting/metallic) compositions show a pronounced surface instability relative to semiconducting materials. Further work is in hand to investigate the underlying causes of this phenomenon, which does not appear to have been noted previously for any oxide system.

4. $Bi_2Sr_2Ca_{n-1}Cu_nO_{4+2n}$ systems

XPS may be used in a similar way to probe contaminant phases occurring at the surfaces of $Bi_2Sr_2Ca_{n-1}Cu_nO_{4+2n}$ (BCSCO) materials. Surfaces of BCSCO materials examined prior to any UHV cleaning procedure again tend to show two features in the O 1s region of the spectrum, with the higher binding energy component enhanced in grazing emission. In this case, corresponding changes are also seen the the Sr 3d, Ca 2p and C 1s (CO_3^{2-}) parts of the spectrum, leading to the inference that $SrCO_3$ and $CaCO_3$ are among the degradation products [1,20,21], although $Sr(OH)_2$ has also been suggested as a product [4,5].

An example of the O 1s and Sr 3d regions for an as-presented (uncleaned) $Bi_2Sr_2CaCu_2O_8$ ceramic is shown in figure 5. As can be seen, the higher binding energy (contaminant) component of the O 1s line is slightly enhanced in grazing emission. The Sr 3d line is more complex, as for a single Sr environment, the line is naturally split by spin-orbit coupling into two closely-spaced components ($3d_{5/2}$ and $3d_{3/2}$). The relative intensities of the two parts of the doublet should be roughly determined by their relative degeneracies , which in this case gives a ratio of 3:2, with the more intense peak at lower binding energy. In figure 5, it can be seen that there is clearly an additional component of the peak to higher binding energy; the feature is a "composite" peak, made up of two features, each consisting of a doublet with a narrow splitting. The net effect is that the contaminant features enhance the high binding energy side of the feature; these features may be removed by annealing inside the spectrometer in an atmosphere of pure oxygen, leading to a single doublet feature, showing

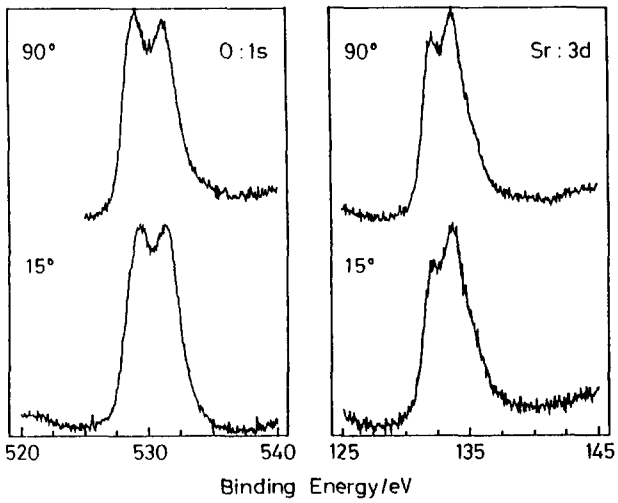

Figure 5. O 1s and Sr 3d XPS of as-presented polycrystalline $Bi_2Sr_2CaCu_2O_{8+x}$. Note the increase in intensity of the high binding energy components on changing from 90° to 15° emission angle relative to the surface.

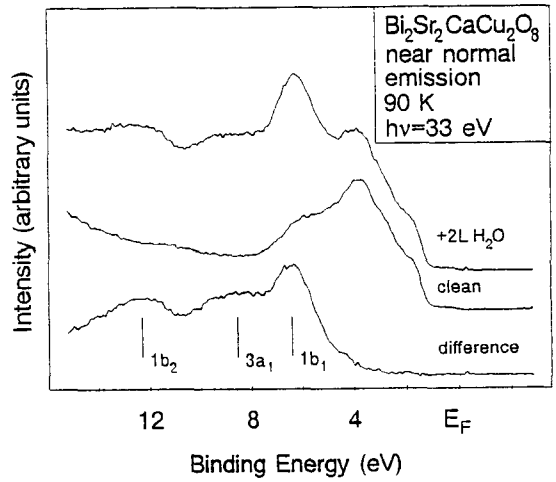

Figure 6. Valence band photoemission spectra of clean and water-dosed single crystal $Bi_2Sr_2CaCu_2O_8$ (001) at 90K. The difference spectrum corresponds to (2L H_2O - clean), where 1L = 1.32×10^{-6} mbar s. Vertical ionisation energies for gas-phase water are also shown, aligned at the $1b_2$ peak positions. Note the absence of any bonding shift of the $3a_1$ level away from its position relative to $1b_1$ in gas phase water [22].

an intensity ratio closer to the expected 3:2 ratio [20]. $CaCO_3$ appears to be present only in cases of quite severe surface contamination [20]. In general, the BCSCO phases appear to be appreciably more stable to degradation than the systems discussed in sections 2 and 3 [20]. In this context, it is interesting to note that the standard free energies of formation, $\Delta G°$ of the alkaline earth carbonate series $CaCO_3$, $SrCO_3$, $BaCO_3$ from the gaseous oxides and CO_2 under standard conditions are -131.4 kJ mol^{-1}, -183.3 kJ mol^{-1} and -215.5 kJ mol^{-1} respectively, reflecting increasing thermodynamic stability of the carbonate as the series is descended. Assuming that the thermodynamic stability of the products formed is a driving force for the degradation reaction, then the higher stability of the BCSCO phases relative to $YBa_2Cu_3O_{7-x}$ and $BaPb_{1-x}Bi_xO_3$ may be partly due simply to the absence of Ba in this compound.

One other feature which undoubtedly plays a part is the layer structures of the BCSCO phases, which leads to strongly anisotropic physical properties. In particular, the two adjacent Bi-O planes of the layer stack have a long interplanar spacing, and are weakly held together. The natural cleavage face of BCSCO is then a (001) face, formed by disruption of the weak bonds between these two planes. BCSCO ceramics and thin films grow naturally with a strong (001) orientation. The (001) face produced by cleaving BCSCO single crystals appears to be fairly unreactive, particularly to the components of the atmosphere involved in the initial stages of degradation, i.e. CO_2 and H_2O. Figure 6 shows some of our earlier work, where a $Bi_2Sr_2CaCu_2O_8$ single crystal was exposed to H_2O at low temperatures [22]. At a temperature of 90 K and low coverage, water remains essentially physisorbed (rather than chemisorbed), as evidenced by the absence of any bonding shift of the $3a_1$ molecular orbital of the adsorbed water. (In cases of chemisorption of water on metal oxides, the $3a_1$ level is shifted to higher binding energy relative to the $1b_1$ and $1b_2$ levels by as much as 1.3 eV [22]. Some shift due to chemisorption is generally apparent for metal oxides, including perovskites, even at low temperature [22].) Although very little experimental work aimed at studying the initial stages of adsorption of atmospheric gases on oxide superconductor surfaces has been carried out (particularly using single crystal substrates), it appears that BCSCO surfaces are less reactive than those of other systems towards molecules such as H_2O [1].

This apparent stability and rather inert character of the BCSCO phases is one of the factors which has contributed to their extensive use in superconducting thin films, wires and tapes. In the case of wires and tapes, this property is doubly important, as in addition to showing an enhanced resistance to degradation, the phases

apparently show rather little reaction when interfaced with metals such as Ag, Cu or Au [23-26].

5. Studies of BCSCO tapes and wires

One of the most commonly used techniques for the production of superconducting wire has been to pack a hollow metal billet with oxide powder, and to draw this into a wire, producing a superconducting core within a metal sheath. Various annealing cycles are then used to optimise the properties of the resultant wire. The metal of choice has generally been silver, as this is believed to be relatively unreactive towards BCSCO, whilst in some way conferring on the superconductor an enhanced resistance to degradation [27]. Silver has also been observed to improve the stability of Y-Ba-Cu-O materials (see e.g. reference [6]). There is therefore some interest in studying the interface between the silver coating and the superconducting core by XPS, in order to investigate the passivating effect of silver on the core material. If this is to be done using real tapes and wires (rather than in model situations where silver is gettered onto BCSCO materials [23,28]) then a facility with high spatial resolution is required in order to image small areas of wire cross-sections. Here, we show some initial results from sections of silver sheathed tape and wire, where the core material is of nominal composition $(Bi_{0.9}Pb_{0.1})_{2.3}Sr_{2.0}Ca_{1.9}Cu_3O_{10+x}$ (i.e. a lead-stabilised BCSCO 2223 phase), provided by National Power PLC (Research and Technology), UK.

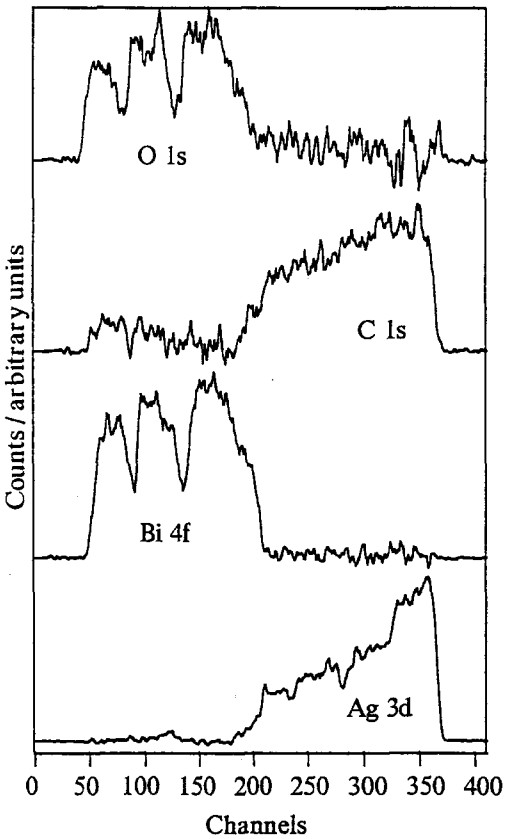

Figure 7. Intensities of O 1s, C 1s, Bi 4f and Ag 3d XPS signals as a function of distance along a 30 μm-wide line scan perpendicular to the interface between the core and the casing for a silver-sheathed tape of composition $(Bi_{0.9}Pb_{0.1})_{2.3}Sr_{2.0}Ca_{1.9}Cu_3O_{10+x}$. The core material lies on the lefthand side of the diagram, and the silver casing on the righthand side. The interface lies at around 200 channels, where one channel corresponds to around 10 μm.

The wires were sectioned using a lubricated diamond saw. Although this had the disadvantage of increasing the level of carbon contamination of the resulting spectra, it was necessary to section the samples in this way to avoid extraneous silver contamination of the core by metal from the sheath dragged across the core by the cutting process. Tapes were prepared by carefully peeling back the top surface of the Ag sheath, to reveal the BCSCO core. XPS were recorded using two spectrometers, a VG ESCASCOPE (which provided elemental maps of the cross-sections at sub-10 μm resolution) and a SCIENTA ESCA 300, which in addition to excellent energy resolution, provided line scans with spatial resolution of the order of 20 - 30 μm.

Figure 7 shows line scans taken across the interface between the silver covering and the core for a tape prepared by rolling an annealed wire material. The diagram shows the intensity of various XPS features (corrected for background intensity) as a line scan is performed crossing the tape - core interface. In this case the width of the advancing line scan is 30 μm, and each channel corresponds to a distance perpendicular to the interface of ≈ 10 μm. Drops in intensity at either end of the scans are artifacts caused by the shadow of the analyser slits on the detector, as the slit width is narrower than the detector. Sudden drops in intensity across the core material, which are reproduced in both the O 1s and Bi 4f scans, are caused by irregularities in the exposed core surface.

It can be seen that the outer Ag surface of the tape is strongly contaminated with carbon and oxygen, as would be expected for a surface exposed to the atmosphere. Strong O 1s and Bi 4f signals are seen from the core, which shows relatively little carbon contamination. The impression that the silver penetrates the core at the interface, gained from the lower trace of figure 7 is slightly misleading. Unless the interface is linear on a 30 μm length scale, and exactly perpendicular to the path of the line scan, an interface between two different elements, A and B will not appear as a step function in the spectra. However, for such an interface, the profiles for elements A and B in the region of the interface should

have a mirror-image relationship to one another (with some overlap at the junction). If there is diffusion of one element into the other phase, the observed profile will be more complex. Given this, the interface between the core and the silver casing appears to be quite abrupt. In particular, there does not appear to have been a noticeable incorporation of Ag into the core material between channels 50 and 200, where the top surface of the tape has been removed. The absence of any appreciable migration of silver into the core in the wire precursors of the tape materials was confirmed from XPS chemical maps of cross-sections of wire (not shown [29]).

A number of photoemission studies of precious metal passivation of superconductor surfaces have been carried out [23-26,28], but these have generally involved the study of a model system where thin layers of the metal are deposited from getter sources onto single crystal BCSCO materials. There is not necessarily any reason to suppose that real wires and tapes will show similar behaviour. The tapes and wires have been subjected to high pressures and temperatures during extrusion and annealing. In addition, the interface between the metal and the superconductor is unlikely to be atomically clean in the real situation. However, our findings are generally in line with the earlier XPS examinations of Ag [23,28] and Au [24] gettered onto BCSCO (001) surfaces, which concluded that the reaction of these metals with the Bi-O plane is rather weak. Recent STM investigations of Ag overlayer growth on the (001) surface suggest that the disruption of the Bi-O and underlying planes initiated by adsorption of silver is quite extensive in the topmost few planes of the structure, but that the main effect is to produce a surface dominated by Bi_2O_3-like clusters (at low Ag coverage) [28]. Our preliminary studies would tend to support this hypothesis, as in some cases we are able to observe a slightly enhanced Bi 4f and O 1s intensity at the interface between the core and the metal in some of our elemental maps of cross-sections of superconducting wire (albeit with a 10μm resolution, rather than the sub-nm resolution of STM) [29]. However, the exact reasons for the passivating effect of silver on superconductor materials remain unclear; further work is in hand to investigate this phenomenon.

6. Conclusions

XPS, used in combination with other spectroscopic techniques is a powerful probe of atmospheric degradation reactions occurring at the surfaces of high temperature superconducting oxides. Much further work needs to be conducted in this area, especially on high quality single crystal samples, where the rate of degradation in UHV may be to some extent controlled, and intergrain contributions may be eliminated. The initial steps in the reactions may then be studied by appropriate dosing experiments.

Carbonate species, which may be detected by XPS, FTIR or Raman spectroscopy are important products of extended degradation for all the systems described. Our work to date tends to indicate that the thermodynamic stability of the final degradation products formed, including the alkaline earth carbonate, may have some influence on the extent of degradation. Structural features of the oxides may also play a part, for example in the case of the BCSCO phases, the relative stability of the preferred Bi-O (001) growth face may be important in hampering the reaction.

In the case of $BaPb_{1-x}Bi_xO_3$, synchrotron-excited photoemission [11] and XPS both appear to indicate a dramatic change in surface reactivity at the metal-to-non-metal transition point, with all metallic compositions being rather susceptible to degradation. The reasons for this are unclear at present, and further work is in hand to see if this phenomenon occurs in other oxide systems where metal-insulator transitions may be induced by chemical doping.

7. Acknowledgements

This work was funded by SERC (UK), with additional support from the Royal Society. We thank Dr S.E. Male of National Power PLC (Research and Technology) for the provision of samples of superconducting tapes and wires.

References

1. M. S. Golden W. R. Flavell and R. G. Egdell, J. Mat. Chem., 1, (1991), 489.
2. Y. Gao, Y. Li, K.L. Merkle, J.N. Mundy, C. Zhang, U. Balachandran and R.B. Poeppel, Mater. Lett., 9, (1990), 347.
3. Y. Gao, K. L. Merkle, C. Zhang, U. Balachandran and R.B. Poeppel, Mat. Lett., 5, (1990), 1363.
4. Sui-Geng Jin, Zheng-Zhong Zhu, Lin-Mei Liu and Yun-Lian Huang, Solid State Commun., 74, (1990), 1087.
5. K. Hotta, H. Magome, Y. Sugiyama, T. Suzuki and H. Hirose, Supercond. Sci. Technol., 4, (1991), 587.
6. T.R. Cummins, R.G. Egdell and G.C. Georgiadis, J. Less-Common Met., 164-165, (1990), 1149.
7. R.G. Egdell, W.R. Flavell and P.C. Hollamby

J. Solid State Chem., 79, (1989), 238.
8. M.P. Seah and W.A. Dench, Surf. Interface Anal., 1, (1979), 2.
9 R.G. Egdell, W.R. Flavell and M.S. Golden, Supercond Sci Technol, 3, (1990), 8.
10 C Kittel, Introduction to Solid State Physics, Wiley, New York, 1976.
11. W.R. Flavell, A. J. Roberts, B.C. Morris, D.R.C. Hoad, I. Tweddell, A. Neklesa, R. Lindsay, G. Thornton, P.L. Wincott and T.S. Turner, Supercond. Sci. Technol., in press.
12. H. Matsuyama, T. Takahashi, H. Katayama-Yoshida, Y. Okabe, H. Takagi and S. Uchida, Phys. Rev. B, 40, (1989), 2658.
13. M. Nagoshi, T. Suzuki, Y. Fukuda, T. K. Ueki, A. Tokiwa, M. Kikuchi, Y. Syono and M. Tachiki, J. Phys.: Cond. Matt., 4, (1992), 5769.
14. R. Itti, I. Tomeno, K. Ikeda, K. Tai, N. Koshizuka and S. Tanaka, Phys. Rev. B, 43, (1991), 435.
15. M.A. Sobolewski, S. Semancik, E.S. Hellman and E.H. Hartford, J. Vac. Sci. Technol., A9, (1991), 2716.
16. A.W. Sleight, J.L. Gillson and B.E. Bierstedt, Solid State Comm, 17, (1975), 27.
17. Y. Khan, K. Nahm, M. Rosenberg and H. Willner, Phys. Stat. Sol. (a), 39, (1977), 79.
18. L Herbeau, M.Sc. Dissertation Thesis, UMIST, 1992.
19. N.E. Ingham, 3rd year U/G report, UMIST, 1991; work in preparation for publication.
20. W.R. Flavell, J.A. Hampson, C. Neeson and R.J.D. Tilley, Supercond. Sci. Technol., 1, (1989), 221.
21 M.S. Golden, D. A. Geeson, S.E. Male and W.R. Flavell, Supercond. Sci. Technol., 2, (1989), 185.
22. W.R. Flavell, J.H. Laverty, D.S.-L. Law, R. Lindsay, C.A. Muryn, C.F.J. Flipse, G.N. Raiker, P.L.Wincott and G. Thornton, Phys. Rev. B., 41, (1990), 11623.
23. D. S. Dessau, Z.-X. Shen, B.O. Wells, W.E. Spicer, R.S. List, A.J.Arko, R.J. Bartlett, Z. Fisk, S.-W. Cheong, D.B. Mitzi, A. Kapitulnik and J.E. Schirber, Appl. Phys. Lett., 57, (1990), 307.
24. P.A.P. Lindberg, Z.-X. Shen, B.O. Wells, D.B. Mitzi, I. Lindau, W.E. Spicer and A. Kapitulnik, Phys. Rev. B, 40, (1989), 8769.
25. B.O. Wells, P.A.P. Lindberg, Z.-X. Shen, D.S. Dessau, I. Lindau, W.E. Spicer, D.B. Mitzi and A. Kapitulnik, AIP/AVS Conf. Proc., 182, (1989), 391.
26. D.M. Hill, H.M. Meyer III, J.H. Weaver, C.F. Gallo and K.C. Goretta, Phys. Rev. B, 38, (1988), 11331.
27. e.g. W. Gao, J. Chen, C. Ow Yang, D. McNabb and J. Vander Sande, Physica C, 193, (1992), 455.
28. Y.S. Luo, Y.-N. Yang and J.H. Weaver, Phys. Rev. B, 46, (1992), 1114.
29. D.R.C. Hoad, W.R. Flavell, I.W. Fletcher and G. Beamson, in preparation.